Neurovascular Unit Model

Documentation for Code "OO-NVU Version 1.2"

A merged NVC model of a neuron, astrocyte, smooth muscle cell, endothelial cell and the mechanical vessel response.

by Emiel van Disseldorp Katharina Dormanns Sanne van der Lelij
Joerik de Ruijter Michelle Louise Goodman Eva Waldhauser
Moritz Burger Kon Zakkaroff Allanah Kenny Tim David*

October 17, 2016

*Corresponding author, Tim.david@canterbury.ac.nz

Contents

1 Release notes

fix references

1.1 Changes to the previous version

1.1.1 Astrocytic Calcium

Farr and David [4] implemented an NVU model based on a simple glutamate efflux into the SC simulating neuronal activity. This model included AC Ca^{2+} variations induced by glutamate production into the SC and the subsequent efflux of K^+ into the PVS from a Ca^{2+} mediated BK channel. In NVU 1.1 this BK channel was not Ca^{2+} mediated and instead approximated by assuming a constant astrocytic Ca^{2+} concentration.

Although the model provided a qualitative description of neurovascular coupling the rate of change of K_p was slow and the dilation of the associated arteriole took too long to reach even small dilations. The K_p at which v_i was maximally hyperpolarised was too high. Therefore NVU version 1.1 did not contain any astrocytic Ca^{2+} or glutamate input as the results were not satisfactory. However various changes were implemented into the model and can be incorporated alongside the NO pathway, producing NVU version 1.2.

These changes included small fixes to the equations of the model by Michelle (e.g. changing a positive to a negative sign). The additional state variables detailing the AC Ca^{2+} model component are found in Table 1.

Variable	Unit	Description
c_k	μM	AC cytosolic Ca^{2+} concentration
s_k	μM	AC Ca^{2+} concentration in the ER
h_k	-	inactivation variable denoting the action of IP_3R that have not been activated by Ca^{2+}
i_k	μM	AC IP_3 concentration
eet_k	μM	Ca^{2+} dependent EET production

Table 1: State variables related to Ca^{2+} in the astrocyte

The ODE for astrocytic Ca^{2+} is:

$$\frac{dc_k}{dt} = B_{cyt}\left(J_{IP3_k} - J_{pump_k} + J_{ERleak_k} + J_{TRPV_k}\right). \tag{1}$$

where the

The ODE for Ca^{2+} in the astrocytic endoplasmic reticulum (internal stores) is:

$$\frac{ds_k}{dt} = -B_{cyt}\frac{(J_{IP3_k} - J_{pump_k} + J_{ERleak_k})}{VR_{ERcyt}}. \tag{2}$$

The inactivation variable denoting the action of IP_3R that have not been activated by Ca^{2+} is:

$$\frac{dh_k}{dt} = k_{on}\left(K_{inh} - (c_k + K_{inh})h_k\right). \tag{3}$$

The astrocytic IP_3 concentration is:

$$\frac{di_k}{dt} = r_h G - k_{deg} i_k. \tag{4}$$

The Ca^{2+} dependent EET production is:

$$\frac{deet_k}{dt} = V_{eet}\max(c_k - c_{k_{min}}, 0) - k_{eet} eet_k. \tag{5}$$

The additional algebraic variables and fluxes are as follows. The flux of Ca^{2+} through the IP_3 mediated channel on the ER is:

$$J_{IP3_k} = J_{max}\left[\left(\frac{i_k}{i_k + K_i}\right)\left(\frac{c_k}{c_k + K_{act}}\right)h_k\right]^3\left(1 - \frac{c_k}{s_k}\right) \tag{6}$$

The flux of Ca^{2+} through the

continue here

The relevant parameters are found in Table 2.

Parameter	Value	Unit	Description
Ca_{decay_k}	0.5	-	Rate of decay of Ca^{2+} in PVS

Table 2: Model parameters related to the astrocytic Ca^{2+} pathway.

1.1.2 TRPV4 channel

Included is a transient receptor potential cation (TRPV4) channel on the astrocytic endfeet adjacent to the PVS. These channels are an important factor in astrocytic sensory and vasoregulatory functions as [3] have shown that certain TRPV4 channels can induce CICR in the endfeet of astrocytes and increase the strength of neurovascular coupling. The flux of Ca^{2+} through the TRPV4 channel is based on the bidirectional model of [14]. In this model vessel dilation activates the TRPV4 channels, allowing an influx of Ca^{2+} from the PVS into the astrocytic cytosol. The two additional state variables to the model are m_k: the open probability of the TRPV4 channel, and c_p: PVS Ca^{2+} concentration (see Table 3).

The ODE for the PVS Ca^{2+} concentration is

$$\frac{dc_p}{dt} = -\frac{J_{TRPV_k}}{VR_{pa}} + \frac{J_{VOCC_k}}{VR_{ps}} - Ca_{decay_k}(c_p - Ca_{min_k}). \tag{7}$$

Variable	Unit	Description
c_p	μM	PVS Ca^{2+} concentration
m_k	-	open probability of TRPV4 channel

Table 3: State variables related to the TRPV4 channel.

Here c_p always decays to the steady state value Ca_{min_p} and J_{VOCC_k} is a voltage operated calcium channel (VOCC) connecting the SMC to the PVS. When the membrane of the SMC hyperpolarises the channel closes.

The ODE for the open probability of TRPV4 channels is:

$$\frac{dm_k}{dt} = \frac{m_{\infty_k} - m_k}{t_{TRPV_k}}. \tag{8}$$

The additional algebraic variables and fluxes are as follows. The flux of Ca^{2+} through the TRPV4 channel is:

$$J_{TRPV_k} = -\frac{1}{2}\frac{G_{TRPV_k} m_k (v_k - E_{TRPV_k}) C_{correction}}{C_{astr_k} \gamma_k r_{buff}} \tag{9}$$

The factor 1/2 is there because there are 2 positive charges for every Ca^{2+} ion [15]. E_{TRPV_k} is the Nernst potential of the TRPV4 channel:

$$E_{TRPV_k} = \frac{RT}{z_{Ca}F} \log\left(\frac{c_p}{c_k}\right). \tag{10}$$

The equilibrium state of the TRPV4 channel is:

$$m_{\infty_k} = \frac{1}{1 + \exp\left(-\frac{\eta - epshalf_k}{\kappa_k}\right)} \frac{1}{1 + H_{Ca_k}} \left(H_{Ca_k} + \tanh\left(\frac{v_k - v_{1,TRPV}}{v_{2,TRPV}}\right)\right), \tag{11}$$

where H_{Ca_k} is an inhibitory term:

$$H_{Ca_k} = \frac{c_k}{\gamma_{Cai}} + \frac{c_p}{\gamma_{Cae}}, \tag{12}$$

and η is the local radial strain on the arteriole:

$$\eta = \frac{R - R_{passive}}{R_{passive}}. \tag{13}$$

The strain on the perivascular endfoot of the AC is approximately equal to local radial strain on the arteriole since the endfoot surrounds the arteriole.

The membrane potential of the AC is modified to include the TRPV4 channel:

$$v_k = \frac{g_{Na_k}E_{Na_k} + g_{K_k}E_{K_k} + \boldsymbol{g_{TRPV_k}m_kE_{TRPV_k}} + g_{Cl_k}E_{Cl_k} + g_{NBC_k}E_{NBC_k} + g_{BK_k}w_kE_{BK_k} - J_{NaK_k}F/C_{correction}}{g_{Na_k} + g_{K_k} + g_{Cl_k} + g_{NBC_k} + \boldsymbol{g_{TRPV_k}m_k} + g_{BK_k}w_k}. \tag{14}$$

The conductance g_{TRPV_k} is calculated using the area of the astrocytic endfeet (similar to the calculation of the conductance of the BK channel at the astrocytic endfeet):

$$g_{TRPV_k} = \frac{G_{TRPV_k}10^{-12}}{A_{ef_k}}, \tag{15}$$

where the conductance is multiplied by 10^{-12} to convert from pS to Ω^{-1} (mho).

The new parameters are found in Table 4.

Parameter	Value	Unit	Description
Ca_{decay_k}	0.5	-	Rate of decay of Ca^{2+} in PVS
Ca_{min_k}	2000	μM	steady state value of Ca^{2+} in PVS
t_{TRPV_k}	0.9	mV	Decay rate of the open probability m_k
G_{TRPV_k}	50	pS	Conductance of TRPV4 channel
$C_{correction}$	10^3	-	Convert from V to mV
C_{astr_k}	40	pF	AC cell capacitance
γ_k	834.3	mV μM^{-1}	scaling factor relating movement of ions to membrane potential
$epshalf_k$	0.1	-	Strain required for half activation of the TRPV4 channel
κ_k	0.1	-	Related to strain and TRPV4 channel
$v_{1,TRPV}$	0.12	mV	Related to voltage gating of TRPV4 channel
$v_{2,TRPV}$	0.013	mV	Related to voltage gating of TRPV4 channel
γ_{Cai}	0.01	μM	Related to Ca^{2+} concentration
γ_{Cae}	200	μM	Related to Ca^{2+} concentration
r_{buff}	0.05	-	Rate of Ca^{2+} buffering at the endfoot compared to the astrocyte body

Table 4: Model parameters related to the TRPV4 channel.

Note that the flux of Ca^{2+} through the TRPV4 channel is buffered at a lower rate r_{buff}, as the channel is located at the astrocytic endfoot and buffering is described by [**?**] in the astrocytic soma. Therefore it is reasonable to assuming buffering at the smaller endfoot of the astrocyte will be at a lower rate.

1.1.3 Nitric Oxide

Nitric oxide (NO) is a neurotransmitter known to act as a potent cerebral vasodilator. It is not produced in advance or stored and due its small size it is able to diffuse widely and readily

in all 3 dimensions and is not limited to local effects, setting it apart from other signalling molecules of the central nervous system. It can rapidly spread even through membranes as it is extremely diffusible in aqueous and lipid environments. However NO has a very short half life as it is an unstable gaseous free radical, limiting its activity temporally [**?**] .

NO is produced in a variety of different tissues. The biochemical reaction that synthesises NO is catalysed by the enzyme family of nitric oxide synthases (NOS): neuronal (nNOS), endothelial (eNOS), and inducible (iNOS), found in neurons, ECs and multiple cell types respectively [**?**]. The literature suggests that the production source and quantity of NO determines its function; NO may either act neuroprotectively by controlling vascular smooth muscle tone and blood flow and hence preventing ischaemic cell injury, or neurotoxically leading to cerebral degeneration [**?**].

The focus of the NO pathway is on NO production by nNOS and eNOS. Both enzymes' activation is mediated by intracellular Ca^{2+} of the NE and EC respectively and eNOS is also activated by blood flow induced wall shear stress (WSS) in cerebral arterioles. NO is able to diffuse rapidly into other compartments. When NO reaches the SMC it interacts with intracellular enzyme activation and regulates SMC relaxation. The dynamics of NO in the NE, AC, SMC and EC are described by using mass balance formulations. The NO concentration in compartment j is:

$$\frac{d[NO]_j}{dt} = p_{NO,j} - c_{NO,j} + d_{NO,j}. \tag{16}$$

$p_{NO,j}$ is the production flux, $c_{NO,j}$ is the consumption flux (i.e. reaction with oxygen or other molecules), and $d_{NO,j}$ is the diffusive flux. Diffusion is assumed to be linear with characteristic distance of $\Delta x = 3.75$ μm between the EC and SMC layers, and $\Delta x = 50$ μm between the NE and SMC layers. The production rate is dependent on the concentration of activated NOS. nNOS and eNOS are thought to be the most influential NO producers, hence we assume NO production in only the NE and EC compartments and no production in the other cell types.

NO synthesis in the NE is catalysed by nNOS in response to glutamate induced calcium influx into the post synaptic neuron and depends on the available concentration of the biochemical substrate L-Arginine (L-Arg) and oxygen (O_2). The nNOS activation is triggered by glutamate in response to neuronal activation. NO production in the EC is catalysed by eNOS dependent on the availability of L-Arg and O_2 and is mediated by WSS.

NO, via its second messenger cGMP, influences the contraction of the SMC (AMp, Mp, AM, M) and the open probability of the SMC K^+ channel w_i. NO activates soluble guanylyl cyclase (sGC) which catalyses the formation of cGMP. cGMP changes the rate constants K_2

and K_5 for the dephosphorylation of Mp to M and AMp to AM (these rate constant were previously set at 0.5 s^{-1} based on Koenigsberger et al. [10]). w_i is shifted to the left by cGMP via the equilibrium state $K_{act_i}(c_{w,i})$ with $c_{w,i}$ as a function of cGMP.

The initial NVU model version 1.1 is extended into version 1.2 by additional mathematical equations that represent production, diffusion and consumption of NO in different cell types, as well as the interaction of NO with other biochemical species and ion channel open probabilities. The model of NVU 1.2 also contains astrocytic Ca^{2+} and a TRPV4 channel. The additional NO pathway equations are found in the appendix of [2] and corresponding additional state variables are detailed in Table 5.

add equations here

Variable	Unit	Description
NO_n	μM	NE NO concentration
NO_k	μM	AC NO concentration
NO_i	μM	SMC NO concentration
NO_j	μM	EC NO concentration
$cGMP$	μM	SMC cGMP concentration
$eNOS$	μM	activated eNOS
$nNOS$	μM	activated nNOS
c_n	μM	NE cytosolic Ca^{2+} concentration
E_b	-	fraction of sGC in the basal state
E_{6c}	-	fraction of sGC in the intermediate form

Table 5: State variables related to the NO pathway

Neuronal stimulation is simulated by an input of both glutamate and K^+ into the SC. The implementation of the NO pathway results in a larger steady state vessel radius, due to a constant supply of vasodilatory NO from the EC and NE. The radius profile also shows a larger and longer response to stimulation. The response of the radius to stimulation can be divided into two components: the fast component in response to the SC K^+ increase (modelled by NVU version 1.1) and the slow component only found with the addition of the NO pathway.

The slower component of the model with the NO signalling pathway is the increase of cGMP in the SMC. This leads to the shift of the open probability of the SMC K^+ channel w_i. The efflux of K^+ from the PVS increases with the opening of the channel so that the PVS K^+ concentration drops at a faster rate. Instead of reaching steady state conditions after

around 100 s, as the model would do if the NO pathway is not included (version 1.1), the SMC membrane potential v_i drops further. Consequently the VOCC channel closes further and the SMC Ca^{2+} concentration decreases. As an overall behaviour the vessel dilates further and returns back to the resting state more slowly.

Hence the SC K^+ release governs the fast onset of vasodilation whilst the NO-modulated mechanisms (increase of SMC cGMP leads to shift in w_i) and the WSS activated NO release from the EC is responsible for maintaining the dilation longer and thus providing more oxygen and glucose to adjacent brain tissue with increased cerebral blood flow. In the resting state the EC provides the major contribution towards vasorelaxation, whereas during neuronal stimulation NO produced by the NE dominates [2].

The radius r in this term is set as constant 25 μm in order to create a reasonable boundary condition at the lumen side of the NVU based on physiological results.

2 Code Structure

The three core classes, the `Astrocyte`, `SMCEC` and `WallMechanics`, correspond to the components of the NVU model, namely the astrocyte model, the SMC and EC model, and the mechanical contraction cell model. For a given model component, all fluxes and ODEs are grouped together in the code of the corresponding class. The `NVU` class uses the three core component classes to collect the state variable and derivatives values and pass them to the `ode15s` solver for stiff problems. All classes in OO-NVU code are subclasses of the MATLAB's `handle` class which makes them appear as reference object to avoid unnecessary object duplication on assignment. Figure 1 shows the public interfaces for all OO-NVU classes.

For a proper OO development and complexity management in the future the Astrocyte, SMCEC and the WallMechanics classes should have a common superclass with the shared interface (at least) and functionality. –Kon

The following features apply to the `Astrocyte`, `SMCEC` and `WallMechanics` classes:

1. The core classes rely on the class constructors to initialise the parameters with the help of the class-specific function parse_inputs(varangin). The constructors also initialise the variable indices, initial conditions and the output indices.

2. In every core class the `rhs` method contains the algebraic and state variables, as well as the corresponding equations.

3. The `shared(self, ~, u)` method, where present, provides the access to the shared algebraic or state variables used as input variables in the other model components where appropriate.

The code in the file `nvu_script.m` provides a number of use-cases for running the NVU model. The code Listing 1 shows an example of setting the options for the ODE solver `ode15s` specifying the `odeopts` parameter, however the code works well with default tolerances. The `simulate()` method of the `NVU` class start the simulation.

Listing 1: Initialisation of the NVU model components.

```
1 odeopts = odeset('RelTol', 1e-03, 'AbsTol', 1e-03, 'MaxStep', 1, ...
      'Vectorized', 1);
2
3 nv = NVU(Astrocyte(), ...
```

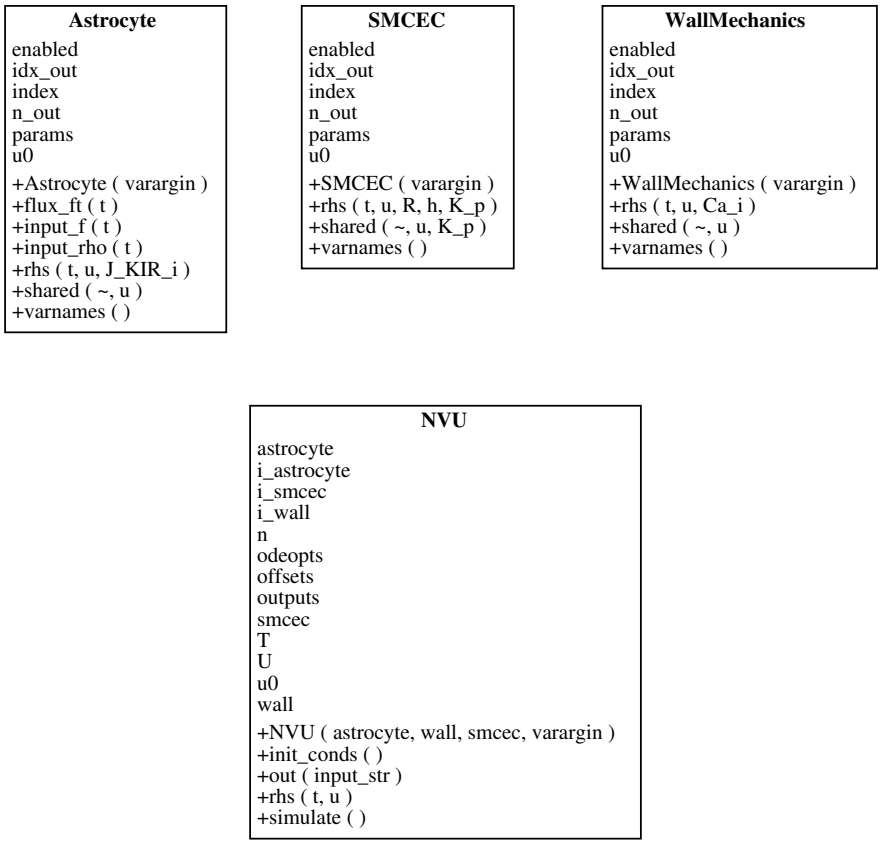

Figure 1: UML class diagram for the OO NVU code.

```
4 WallMechanics(), ...
5 SMCEC('J_PLC', 0.18), ...
6 'odeopts', odeopts);
7
8 nv.simulate()
```

3 Introduction

3.1 Neurovascular Unit

The cerebral cortex, a highly complex component of the human brain and part of the grey matter (*substantia grisea*), mainly consists of neurons (NEs), unmyelinated axons and glial cells such as astrocytes (ACs). It forms the outer layer of *cerebrum* and *cerebellum* and is veined with capillary blood vessels that provide the brain tissue with glucose and oxygen (Shipp [13]). These arterioles are surrounded by endothelial cells (ECs) that form a thin layer on the interior surface of arterioles (*intima*). The outer layer of the arteriole consists of smooth muscle cells (SMCs), which are aligned in circumferential direction. They define the contractile unit of the vessel and regulate its diameter by contraction and dilation.

A neurovascular unit (NVU) defined in this research includes one cell of each of the described types and is graphically pictured in Figure 3.

Each of the cell types and the spaces in between play an important role within the process of neurovascular coupling (NVC, see Section 3.2). The synaptic cleft (SC) is the space between an axon terminal and dendrite of two different NEs in which neurotransmitters are released. It is enclosed by the star-shaped AC that can take up released neurotransmitters. Protoplasmic ACs are polarized cells which can temporarily buffer extracellular K^+, which is one of the key mechanisms within NVC. The astrocytic endoplasmatic reticulum (ER), an isolated space in the cytosol, contains IP_3-sensitive Ca^{2+} channels, which can release Ca^{2+}-ions into the cytosol. The perivascular space (PVS) is located between the end feet of an AC and the arteriole. In the PVS, ion exchange occurs between the arterial wall and the AC. The ECs form a monolayer on the luminal side of the vessel in which all cells are aligned in the direction of the flow. It prevents passive diffusion of bigger molecules, while small ones, such as O_2, Ca^{2+} or IP_3, can pass through. It also functions as an active organ sensing wall shear stress which plays an important role in the NO-mediated pathway. Together with the SMC layer the endothelium forms the blood brain barrier (BBB), the physical frontier between brain tissue and blood vessel. SMC contraction occurs by actin and myosin filaments forming cross-bridges. The rate of contraction is dependent on the SMC cytosolic Ca^{2+} concentration.

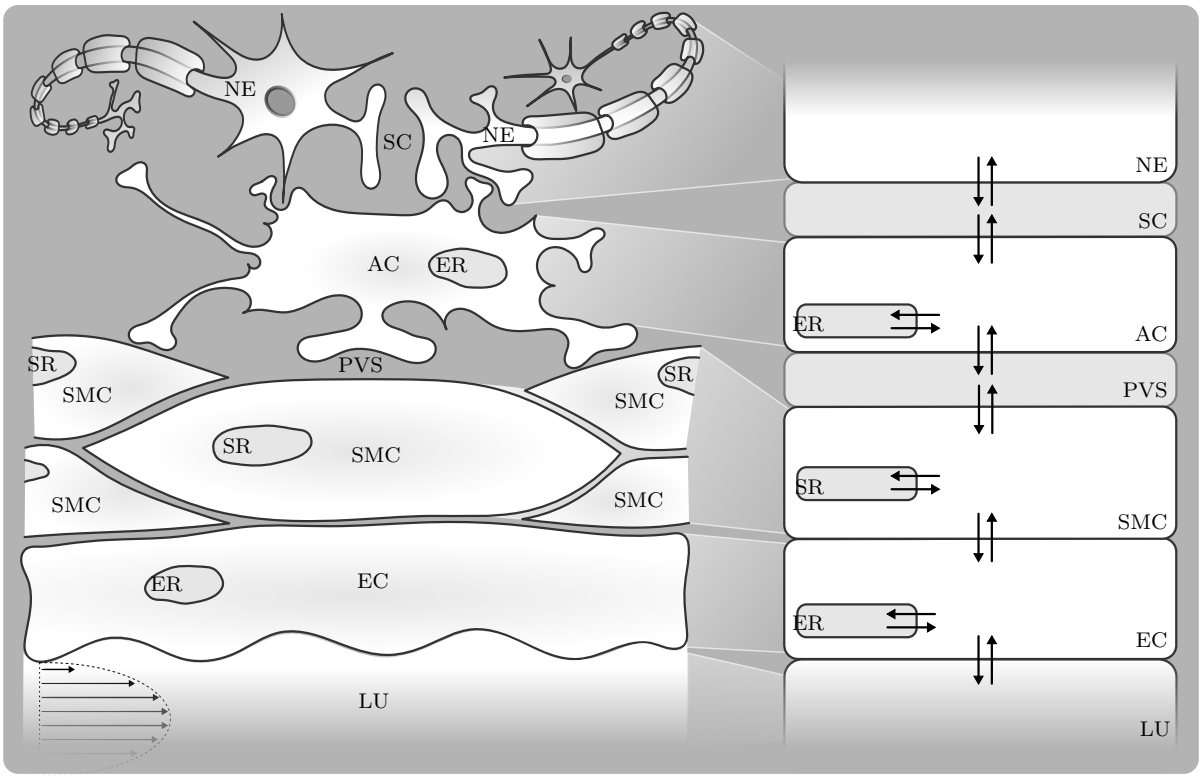

Figure 2: **Overview of different cells and domains that form a neurovascular unit.** NE - Neuron, SC - Synaptic Cleft, AC - Astrocyte, ER - Endoplasmic Reticulum, PVS - Perivascular Space, SMC - Smooth Muscle Cell, SR - Sarcoplasmic Reticulum, EC - Endothelial Cell, LU - Lumen with indicated blood flow. Intercellular communication via the exchange of ions is indicated by arrows.

3.2 Neurovascular Coupling

Neurovascular coupling (NVC), or functional hyperaemia, describes the local vasodilation and -contraction due to neuronal activation. The change in the vessel diameter (vasoreactivity) controls the blood flow and thereby the cerebral supply of oxygen and glucose.

Each cell type plays an important specific role during the process of NVC. Communication between cells is based on an exchange of ions through pumps and channels. These ion fluxes contribute to changes in cytosolic and intercellular species concentration and cell membrane potentials.

There are several pathways that can lead to vasocontraction or -dilation and are mediated by different signalling molecules, such as K^+, Ca^{2+}, EET, NO and 20-HETE. Neurotransmitters are released by the NE into the SC and can bind to receptors on dendrites of other

neurons and astrocytes. This leads to a cascade of chemical reactions and the opening and closing of ion channels which influences the fluxes and concentrations.

3.3 Mathematical Approach

The physiological models are based on a set of differential equations that describe the mass conservation of ions and molecules passing from one cell or domain to another. The simulations describe time-dependent ion fluxes and changes in membrane potential modelled by reaction rates that describe the kinetics which are physiologically validated by experimental data from the literature. This approach assumes homogeneous behaviour of a variable in a certain subdomain i.e. the spatial gradient of a variable in every subdomain is negligible.

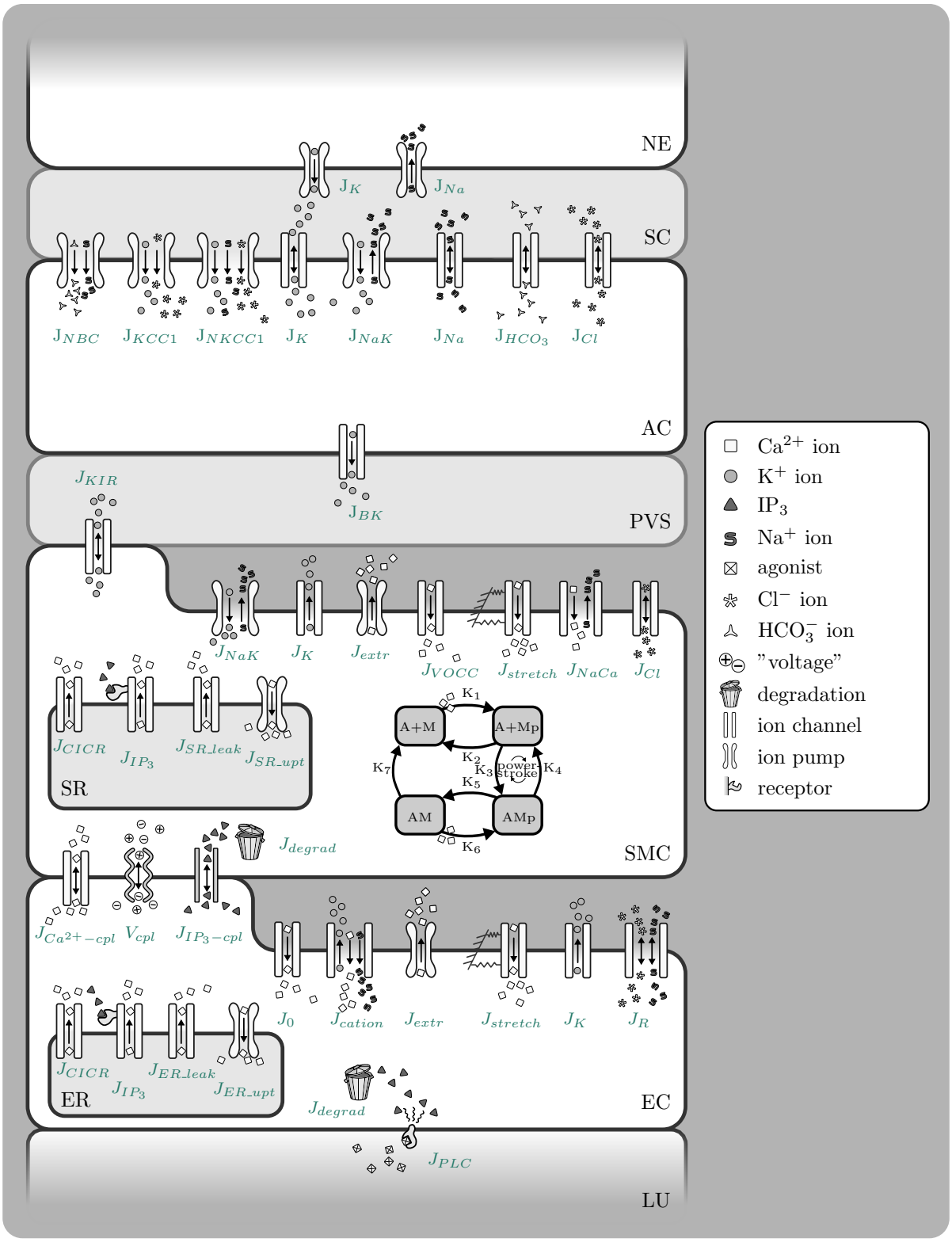

Figure 3: **Overview of model.** NE - Neuron, SC - Synaptic Cleft, AC - Astrocyte, ER - Endoplasmic Reticulum, PVS - Perivascular Space, SMC - Smooth Muscle Cell, SR - Sarcoplasmic Reticulum, EC - Endothelial Cell, LU - Lumen.

4 Existing Models

The present mathematical model is the first of its kind, leading the way in modelling the whole neurovascular coupling process. Starting with the neuronal activation we build up to the response in vessel diameter, utilizing all cell types and crucial pathways. It is based on three existing models.

- **The Astrocyte Model** - describes the crucial biochemical processes within the astrocyte (AC, Østby et al. [12], reviewed by Donk and Kock [1]).
- **The SMC and EC Model** - describes the behaviour and the main ion fluxes within the smooth muscle cell (SMC) and endothelium cell (EC). This model is based on that of Koenigsberger et al. [10].
- **The Contraction and Mechanical Model** - describes the relationship between the cytosolic calcium (Ca^{2+}) concentration in the SMC and the contraction and dilation of the SMC by a myosin phosphorylation and cross-bridge based on the models of **?**] and Kelvin Voigt.

4.1 The Astrocyte Model

During neural activity, K^+ is released into the synaptic cleft (SC) by active neurons (NEs). In the astrocyte model, this is implemented by an influx of K^+ (J_{K_s}) with a corresponding Na^+ uptake by the neuron (J_{Na_s}, Figure 4). The increase of K^+ in the SC results in an increased K^+ uptake by the AC which consequently undergoes depolarization. This results in a K^+ efflux from distant portions of the cell. Since most of the K^+ conductance of ACs is located at the end-feet, the outward current-carrying K^+ would flow out of the cell largely through these locations. Consequently, the K^+ is 'siphoned' to the end-feet of the astrocyte and released into the perivascular space (PVS) which leads to an increase of K^+ in the PVS. This K^+ release leads to a repolarization of the membrane voltage and is the input signal for the second (SMC & EC) part of this model.

The AC model contains different types of active and passive ion channels. These ion channels and pumps are captured in a set of differential equations to describe the conservation of mass for the corresponding species concentrations in the SC, the AC and the PVS. The ion channels for potassium (J_{KCC1}, J_{NKCC1}, J_K, J_{NaK} and J_{BK}), sodium (J_{NBC}, J_{NKCC1}, J_{NaK} and J_{Na}), chloride (J_{KCC1}, J_{NKCC1} and J_{Cl}) and bicarbonate (J_{HCO_3}) are included.

Note that the bicarbonate and chlorine fluxes are coupled with the Na^+ and K^+ fluxes to obtain a neutral in- or efflux membrane voltage-wise.

The release of glutamate from the neuron in the synaptic cleft is simulated by creating a smooth pulse function ρ that describes the ratio of bound to total glutamate receptors on the synapse end of the astrocyte. This induces an IP_3 release into the cell, causing the release of Calcium from the ER into the cytosol, which then leads to the production of EET. The K^+ release into the PVS is controled by the BK-channels. The opening of the BK-channels is regulated by the membrane voltage, as wel as the EET and Ca^{2+} concentration.

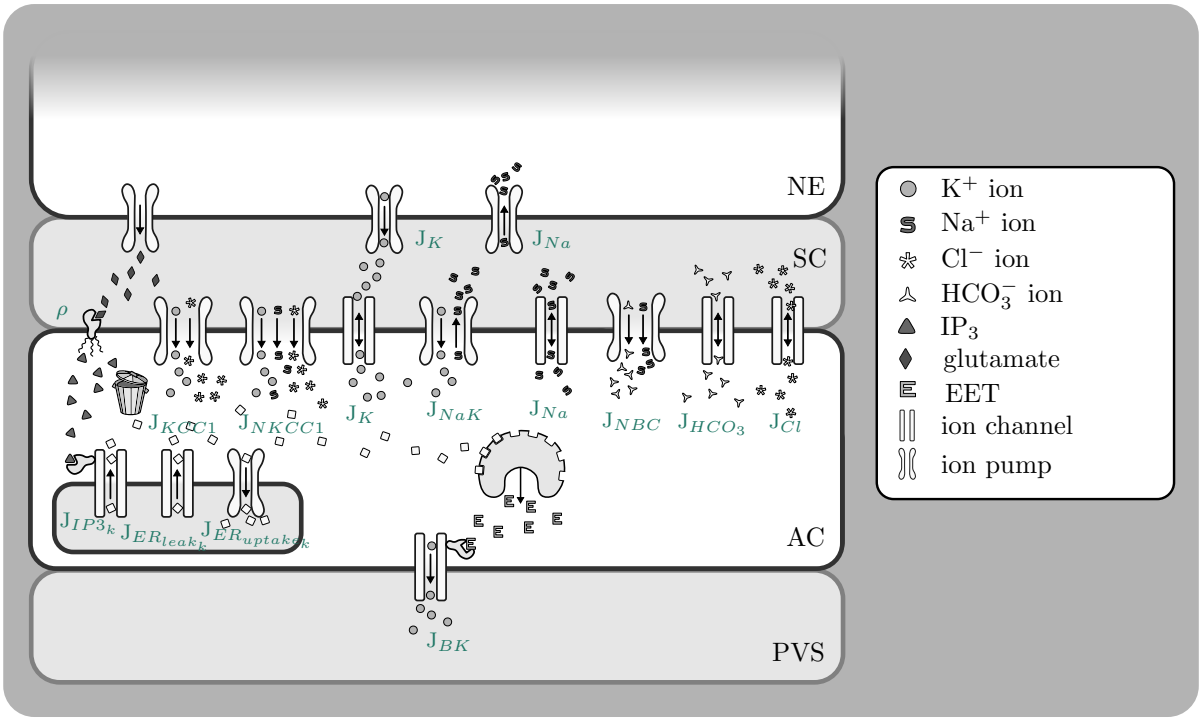

Figure 4: **Illustration of the astrocyte model.** All modelled fluxes are pictured, note that the indices (k - Astrocyte (AC), s - Synaptic Cleft (SC), p - Perivascular Space (PVS)) are left out for clarity reasons.

4.1.1 Input Signal

In this model, a neuronal excitation was mimicked by an efflux of K^+ into the synaptic cleft (SC) and a simultaneous equal influx of Na^+ into the neuron from the SC (Østby et al. [12], see equations in section 5.1). The time-dependent input signal ($f(t)$, see figure 5) starts at $t = 200s$ and ends at $t = 210s$. To estimate the profile $f(t)$ of the K^+ efflux/Na^+ influx, it is assumed that the K^+ efflux has a shape of a beta distribution with the governing parameters α and β such that the profile is optimized according to two criteria [12]:

1. The time from the start until the attaining maximum level of the K^+ concentration in the SC is 5s.
2. The level of the K^+ concentration in the SC at $t = 30$s is 60% of the minimal level.

These two criteria take into account that β is set at a value of $\beta = 5$.

In order to enhance the maximum K^+ level in the SC to reach the order of magnitude proposed by Filosa [5], the amplitude of the input signal $f(t)$ is scaled up by the value F_{input}. The quantity of K^+ ions pumped into the AC can be derived by taking the integral of the flux $k_c f(t)$ over time, where k_c is a constant that relates the input signal $f(t)$ to the K^+ influx.

The amount of released ions are slowly buffered back by the neuron after the input signal terminates. This is modelled by a decay constant within the time interval $230s \leq t \leq 240s$. The integral of this block function is the same as the integral of the beta distribution in order to return to the baseline.

Beside this neuronal input signal, the NKCC1 and KCC1 co-transporters are only enabled when the neuronal ion release and spatial buffering are applied. With both parameters added, the behaviour is modelled by a block function with the value $-F_{input}$ with a default value of zero (Figure 5).

4.1.2 Scaling

The flux equations used in the AC model are based on the model of Østby et al. [12]. Their intention was to look at the volume changes of the AC and SC, therefore the volumes of both are variables in this model and all fluxes are scaled by a volume-surface ratio (R_k and

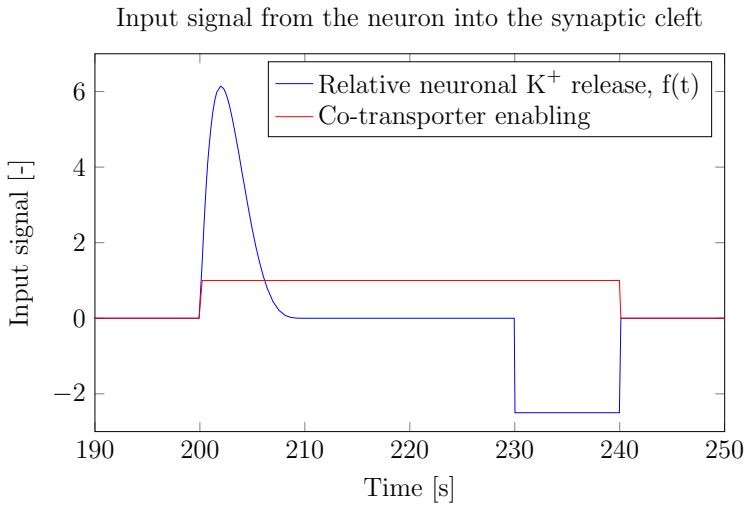

Figure 5: **The input signals used in the astrocyte model.** The K^+ efflux modelled by a beta distribution and buffered back afterwards (blue). The NKCC1 and KCC1 co-transporters are enabled when the neuronal ion release and spatial buffering is applied, modelled by a block function (red).

R_s, see Equations 22 and 23, respectively). It is assumed that the sum of the volumes of the AC and SC is a constant (R_{tot}). Due to osmotic pressure, the volume changes. We could show that the changes are comparatively small in our model and it would be justifiable to leave out the scaling factors. However, at the moment they are included because the given fluxes of Østby et al. [12] are scaled by the volume-surface ratio. It should be considered in future versions to eliminate the scaling factors by multiplying the fluxes with an adequate constant.

4.2 SMC and EC Model

The SMC and EC model is based on the work of Koenigsberger et al. [10], see Figure 6. This model is extended by adding an inward-rectifier potassium (KIR) channel in the SMC (J_{KIR}, [5]) in order to create a connection between the Astrocyte model and the SMC and EC model.

The input signal for this model is the K^+ concentration in the PVS which is increased by the efflux of astrocytic potassium after neuronal activity.

The raise in K^+ in the PVS activates the KIR channel on the SMC, causing them to open extruding more potassium into the PVS. This efflux of K^+ hyperpolarizes the SMC membrane and causing the voltage-operated Ca^{2+} channels to close, preventing the influx of

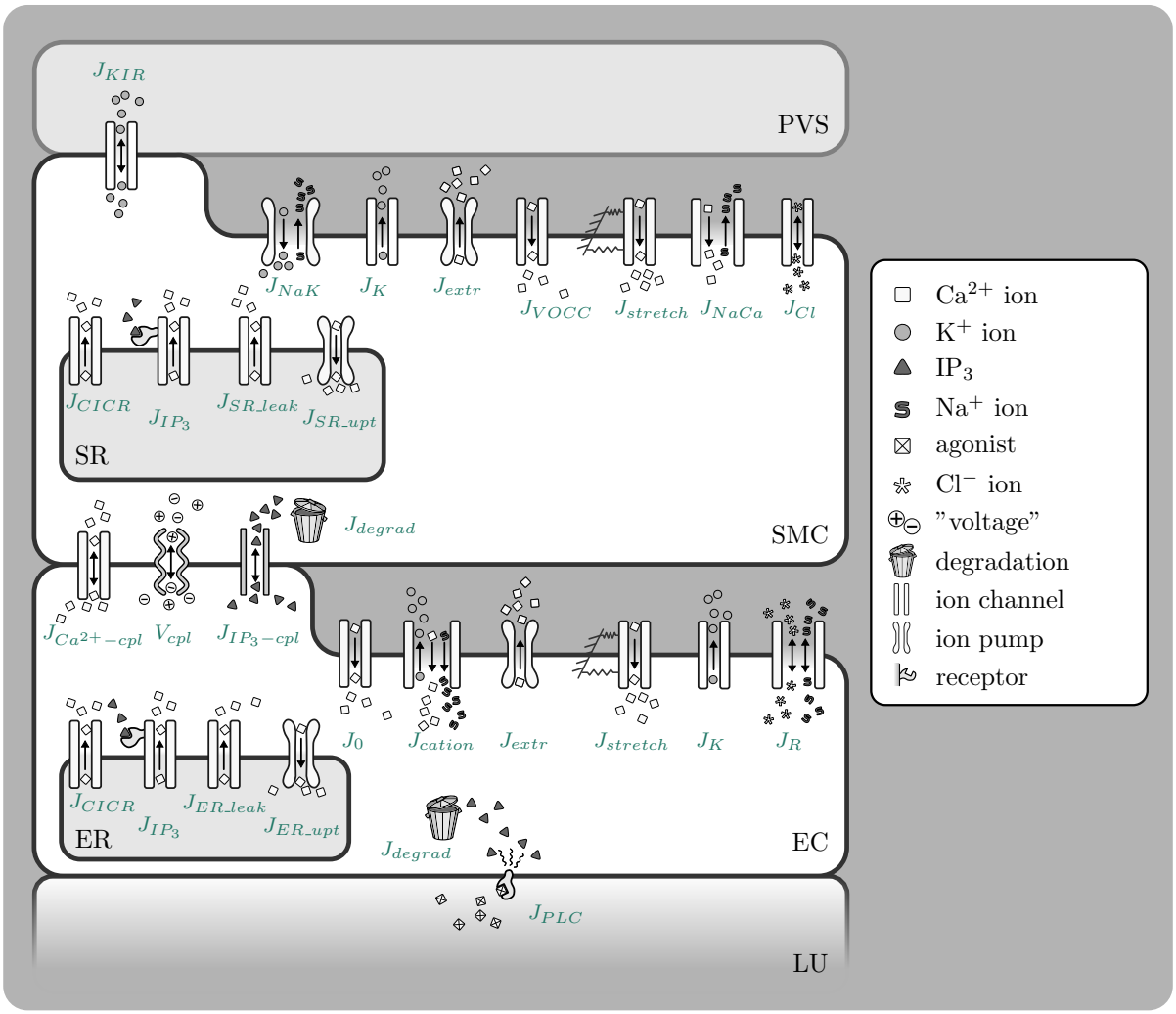

Figure 6: **Illustration of the SMC and EC model.** All modelled fluxes are pictured, note that the indices (k - Astrocyte (AC), s - Synaptic Cleft (SC), p - Perivascular Space (PVS)) are left out for clarity reasons.

Ca^{2+} into the SMC cytosol.

The cytosolic Ca^{2+} concentrations in the SMC and EC and that in the sacroplasmatic reticulum (SR) and endoplasmatic reticulum (ER), respectively, are described by a set of differential equations. In- and effluxes of K^+ are given by the following ion channel and pumps: J_{KIR}, J_{NaK} and J_K. Ca^{2+} leaves the SR via the channels: J_{CICR}, J_{IP_3} and J_{SR_leak} and enters it by J_{SR_upt}. The in- and efflux of Ca^{2+} are modelled with J_{extr}, J_{VOCC}, $J_{stretch}$ and J_{NaCa}. Note that these fluxes link the cytosol with the extracellular matrix. Here again,

a chloride pump is included, J_{Cl}, to return to the resting membrane potential.

Physiologically, ECs and SMCs are connected by gap junctions that allow an intercellular exchange of molecules and voltage. Koenigsberger et al. [10] include the coupling factors $J^{EC-SMC}_{Ca^{2+}-cpl}$, V^{EC-SMC}_{cpl} and $J^{EC-SMC}_{IP_3-cpl}$ for Ca^{2+}, voltage and IP_3 coupling, respectively. The strength of the coupling can be changed in the code with the variable $CASE$.

Inositol triphosphate (IP_3) is an important messenger molecule. It's production, in the endothelium, is triggered by agonist binding onto membrane receptors. IP_3 mediates the J_{IP_3} channel, situated between the reticulum and cytosol. The production rate of IP3 is a constant over time and can be changed by altering the variable J_{PLC} within the mathematical model .

Note that the model of Koenigsberger et al. [10] already includes Ca^{2+}-buffering in the SMC and EC.

4.3 Contraction and Mechanical Model

4.3.1 Contraction Model

The contraction and mechanical part of the model is based on the model of **?**], which describes the formation of cross bridges between the myosin and actin filaments (Figure 7). This is coupled with a Kelvin-Voigt model that is used to describe the visco-elastic behaviour of the arterial wall (Figure 8).

The Ca^{2+} concentration in the SMC is the input signal for the cross bridge model of **?**]. The model uses four possible states for the formation of myosin: free nonphosphorylated cross bridges (M), free phosphorylated cross bridges (Mp), attached phosphorylated cross bridges (AMp) and attached dephosphorylated latch bridges (AM). The dynamics of the fraction of myosin in a particular state is given by four differential equations.

The active stress of the SMC is directly proportional to the fraction of attached cross bridges (AM and AMp). Using this model the relation between the cytosolic Ca^{2+} concentration and the active stress of the SMC can be derived.

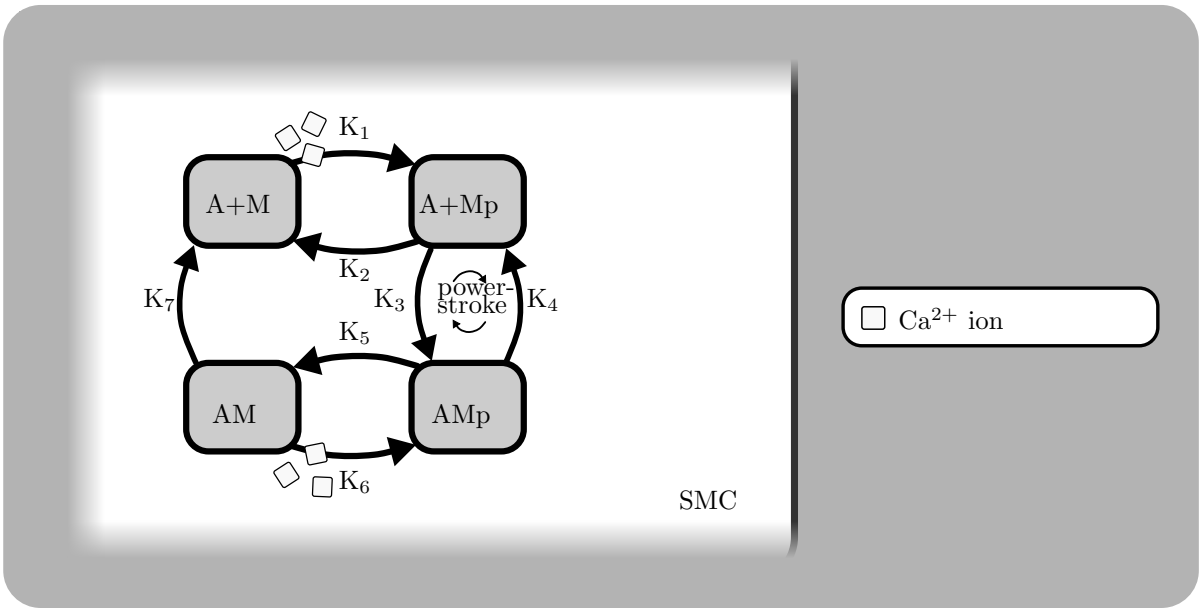

Figure 7: **Illustration of the contraction model within the smooth muscle cell.**

4.3.2 Mechanical Model

The fraction of attached myosin cross bridges is the input signal for the visco-elastic mechanical model (Kelvin Voigt, Figure 8) which describes the changes in radius over time. The pressure inside the vessel wall is taken as a constant and the circumferential stress is calculated using the Laplacian law.

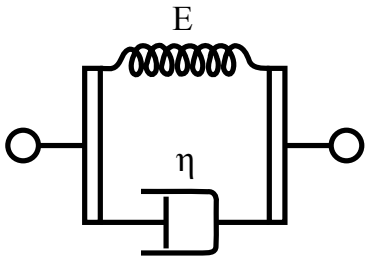

Figure 8: **Schematic overview of a Kelvin Voigt model.**

The Young's modulus and initial radius of the vessel wall is divided into an active and a passive part and is a function of the attached myosin cross-bridges. The active and passive Young's modulus are based and fitted on experimental data of **?**] which is shown in Figure 9.

Figure 9 shows that the initial radius (R_0) decreases when the fraction of attached myosin cross bridges (F) are increased (the intersection with the x-axis). The figure also shows that

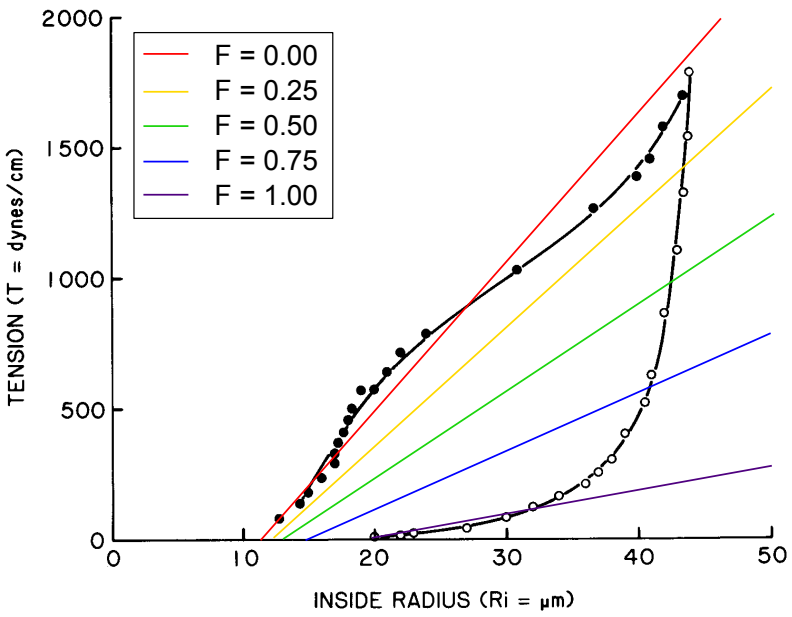

Figure 9: **Linearisation for the Young's modulus and initial radius on the data of ?] for different values of F.**

the Young's modulus, represented by the slope of the lines in the tension-strain graph, increases when F increases. The linearisations of the Young's modulus can be described by:

$$T = \frac{\Delta T}{\Delta R}(R - R_0) \ , \tag{17}$$

where T is the tension of the vessel and $\frac{\Delta T}{\Delta R}$ is the slope of the linearisations in Figure 9.

4.4 Merging of All Models

The Astrocyte model and the SMC and EC model are linked by the SC and the PVS. The K^+ input signal of the neuron is pumped into the SC and taken up afterwards by the AC. The most important ion pumps and channels in this process are the K^+ channels in the neuron which releases the K^+ input, the Na^+/K^+ pump and K^+ channel in the AC which pump the released K^+ into the AC. The result of this is an efflux of K^+ at the end feet of the astrocyte using the BK-channel. Consequently, the membrane voltage of the astrocyte re-polarizes and the K^+ concentration in the PVS increases. This increased K^+ concentration activates the KIR channel in the SMC and start to pump out more K^+ from the SMC into the PVS. The increased efflux of K^+ hyperpolarises the SMC membrane voltage and as a result of that the VOCC closes and prevents the influx of Ca^{2+} into the SMC. Summarising, the neuronal input signal leads to a decrease of Ca^{2+} influx by the VOCC channels and therefore a decrease of the intracellular Ca^{2+} concentration. This leads to a decreased fraction of attached myosin bridges in the Hai and Murphy [8] model, resulting in vessel dilation in the visco-elastic mechanical model. An overview of the whole model is shown in Figure 10.

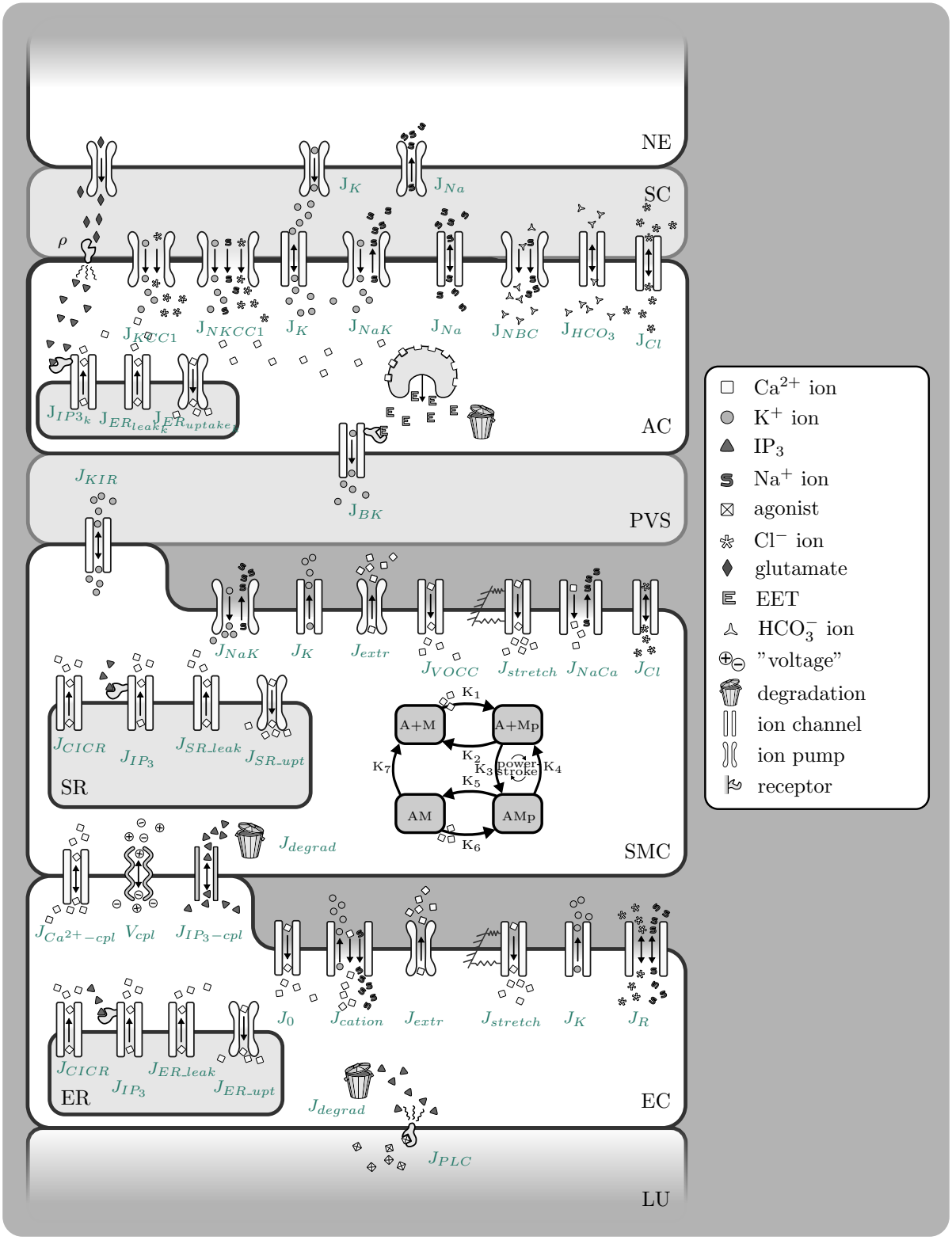

Figure 10: **All Models.**

5 Equations

Some units need to be corrected in this documentation!

add equations for NO in each section, add astrocyte calcium and trpv4 equations to that section, add glutamate signal

5.1 The Neuron and Astrocyte Model

Input signals

Neuronal K^+ input signal (dim.less):

$$f_{\mathrm{K/Na}}(t) = \begin{cases} F_{\mathrm{input}} \dfrac{(\alpha_n + \beta_n - 1)!}{(\alpha_n - 1)!(\beta_n - 1)!} \left(\dfrac{1 - (t - t_0)}{\Delta t_2} \right)^{\beta_n - 1} \left(\dfrac{t - t_0}{\Delta t_2} \right)^{\alpha_n - 1}, & \text{for } t_0 \leq t < t_1 \\ -F_{\mathrm{input}}, & \text{for } t_2 \leq t \leq t_3 \\ 0, & \text{otherwise} \end{cases} \tag{18}$$

End of neuronal pulse (s):

$$t_1 = t_0 + \Delta t \tag{19}$$

Start of back-buffering (s):

$$t_2 = t_0 + \Delta t_1 \tag{20}$$

End of back buffering (s):

$$t_3 = t_1 + \Delta t_1 \tag{21}$$

F_{input}	amplitude scaling factor	2.5	ME[1]
α_n	beta distribution constant	2	ME
β_n	beta distribution constant	5	ME
t_0	start of neuronal activation	400 s	ME
Δt_1	length of neuronal activation	200 s	ME
Δt_2	time-scaling factor	10 s	[12]

1

[1]Model Estimation

Scaling

AC volume-area ratio (in m):

$$\frac{\mathrm{d}R_k}{\mathrm{d}t} = L_p([\mathrm{Na}^+]_k + [\mathrm{K}^+]_k + [\mathrm{Cl}^-]_k + [\mathrm{HCO}_3^-]_k - [\mathrm{Na}^+]_s - [\mathrm{K}^+]_s - [\mathrm{Cl}^-]_s - [\mathrm{HCO}_3^-]_s + \frac{X_k}{R_k}) \tag{22}$$

SC volume-surface ratio (in m):

$$R_s = R_{\mathrm{tot}} - R_k \tag{23}$$

L_p	total water permeability per unit area of the astrocyte	2.1×10^{-9} m µM^{-1}s^{-1}	[12][2]
X_k	Number of negatively charged impermeable ions trapped within the astrocyte divided by the astrocyte membrane area	12.41×10^{-3} µM m	[12]
R_{tot}	Total volume surface ratio AC + SC ($(V_{sc}+V_k)/A_k$)	8.79×10^{-8} m	[12][2]
A_k	characteristic exchange surface area	3.7×10^{-9} m^2	[12][3]

Conservation Equations

Synaptic Cleft

K^+ concentration in the SC (times the SC volume-area ratio R_s; in µM m):

$$\frac{\mathrm{d}N_{\mathrm{K},s}}{\mathrm{d}t} = k_C f(t) - \frac{\mathrm{d}N_{\mathrm{K},k}}{\mathrm{d}t} - J_{\mathrm{BK},k}\,; \quad [\mathrm{K}^+]_s = \frac{N_{\mathrm{K},s}}{R_s} \tag{24}$$

Na^+ concentration in the SC (times the SC volume-area ratio R_s; in µM m):

$$\frac{\mathrm{d}N_{\mathrm{Na},s}}{\mathrm{d}t} = -k_C f(t) - \frac{\mathrm{d}N_{\mathrm{Na},k}}{\mathrm{d}t}\,; \quad [\mathrm{Na}^+]_s = \frac{N_{\mathrm{Na},s}}{R_s} \tag{25}$$

HCO_3 concentration in the SC (times the SC volume-area ratio R_s; in µM m):

$$\frac{\mathrm{d}N_{\mathrm{HCO_3},s}}{\mathrm{d}t} = -\frac{\mathrm{d}N_{\mathrm{HCO_3},k}}{\mathrm{d}t}\,; \quad [\mathrm{HCO}_3^-]_s = \frac{N_{\mathrm{HCO_3},s}}{R_s} \tag{26}$$

k_C	Input scaling parameter	7.35×10^{-5} µM m s^{-1}	[12]

[2] corrected value/unit obtained from `CellML`

[3] corrected value/unit obtained from communication with author

Astrocyte

K^+ concentration in the AC (times the AC volume-area ratio R_k; in µM m):

$$\frac{\mathrm{d}N_{\mathrm{K},k}}{\mathrm{d}t} = -J_{\mathrm{K},k} + 2J_{\mathrm{NaK},k} + J_{NKCC1_k} + J_{KCC1_k} - J_{\mathrm{BK},k}\,; \quad [\mathrm{K}^+]_k = \frac{N_{\mathrm{K},k}}{R_k} \tag{27}$$

Na^+ concentration in the AC (times the AC volume-area ratio R_k; in µM m):

$$\frac{\mathrm{d}N_{\mathrm{Na},k}}{\mathrm{d}t} = -J_{\mathrm{Na},k} - 3J_{\mathrm{NaK},k} + J_{NKCC1_k} + J_{\mathrm{NBC},k}\,; \quad [\mathrm{Na}^+]_k = \frac{N_{\mathrm{Na},k}}{R_k} \tag{28}$$

HCO_3 concentration in the AC (times the AC volume-area ratio R_k; in µM m):

$$\frac{\mathrm{d}N_{\mathrm{HCO_3},k}}{\mathrm{d}t} = 2J_{\mathrm{NBC},k}\,; \quad [\mathrm{HCO}_3^-]_k = \frac{N_{\mathrm{HCO_3},k}}{R_k} \tag{29}$$

Cl concentration in the AC (times the AC volume-area ratio R_k; in µM m):

$$\frac{\mathrm{d}N_{\mathrm{Cl},k}}{\mathrm{d}t} = \frac{\mathrm{d}N_{\mathrm{Na},k}}{\mathrm{d}t} + \frac{\mathrm{d}N_{\mathrm{K},k}}{\mathrm{d}t} - \frac{\mathrm{d}N_{\mathrm{HCO_3},k}}{\mathrm{d}t}\,; \quad [\mathrm{Cl}^-]_k = \frac{N_{\mathrm{Cl},k}}{R_k} \tag{30}$$

Open probability of the BK channel (non-dim.):

$$\frac{\mathrm{d}w_k}{\mathrm{d}t} = \phi_w\,(w_\infty - w_k) \tag{31}$$

Perivascular Space

K^+ concentration in the PVS (in µM):

$$\frac{\mathrm{d}K_p}{\mathrm{d}t} = \frac{J_{\mathrm{BK},k}}{R_k R_{pk}} + \frac{J_{\mathrm{KIR},i}}{R_{ps}} - R_{\mathrm{decay}}([\mathrm{K}^+]_p - [\mathrm{K}^+]_{p,\mathrm{min}}); \tag{32}$$

R_{pk}	Volume ratio of PVS to AC	10^{-3} [-]	[11]
R_{ps}	Volume ratio of PVS to SMC	10^{-3} [-]	[11]
R_{decay}	Decay rate	0.05 s^{-1}	M.E.
$[\mathrm{K}^+]_{p,\mathrm{min}}$	min K^+ concentration	3×10^3 µM	M.E.

Fluxes

K^+ flux (times the AC volume-area ratio R_k; in $\mu\mathrm{M\,m\,s}^{-1}$):

$$J_{\mathrm{K},k} = \frac{g_{K_k}}{F}(v_k - E_{\mathrm{K},k}) \tag{33}$$

Na^+ flux (times the AC volume-area ratio R_k; in $\mu M\,m\,s^{-1}$):

$$J_{\mathrm{Na},k} = \frac{g_{Na_k}}{F}(v_k - E_{\mathrm{Na},k}) \tag{34}$$

Na^+ and HCO_3 flux through the NBC channel (times the AC volume-area ratio R_k; in $\mu M\,m\,s^{-1}$):

$$J_{\mathrm{NBC},k} = \frac{g_{\mathrm{NBC},k}}{F}\,(v_k - E_{\mathrm{NBC},k}) \tag{35}$$

Cl and K^+ flux through the KCC1 channel (times the AC volume-area ratio R_k; in $\mu M\,m\,s^{-1}$):

$$J_{\mathrm{KCC1},k} = C_{input}\frac{g_{\mathrm{KCC1},k}}{F}\frac{R_{\mathrm{gas}}T}{F} ln\left(\frac{[\mathrm{K}^+]_s[\mathrm{Cl}^-]_s}{K_k[\mathrm{Cl}^-]_k}\right) \tag{36}$$

Na^+, K^+ and Cl flux through the NKCC1 channel (times the AC volume-area ratio R_k; in $\mu M\,m\,s^{-1}$):

$$J_{\mathrm{NKCC1},k} = C_{input}\frac{g_{\mathrm{NKCC1},k}}{F}\frac{R_{\mathrm{gas}}T}{F} ln\left(\frac{Na_s[\mathrm{K}^+]_s{[\mathrm{Cl}^-]_s}^2}{Na_k K_k{[\mathrm{Cl}^-]_k}^2}\right) \tag{37}$$

Flux through the sodium potassium pump (times the AC volume-area ratio R_k; in $\mu M\,m\,s^{-1}$):

$$J_{\mathrm{NaK},k} = J_{\mathrm{NaK,max}}\frac{{Na_k}^{1.5}}{{Na_k}^{1.5} + {K_{\mathrm{Na},k}}^{1.5}}\frac{[\mathrm{K}^+]_s}{[\mathrm{K}^+]_s + K_{\mathrm{K},s}} \tag{38}$$

K^+ flux through the BK channel (times the AC volume-area ratio R_k; in $\mu M\,m\,s^{-1}$):

$$J_{\mathrm{BK},k} = \frac{g_{\mathrm{BK},k}}{F} w_k\,(v_k - E_{\mathrm{BK},k}) \tag{39}$$

Specific ion conductance of the BK channel ($\Omega^{-1}m^{-2}$):

$$g_{\mathrm{BK},k} = \frac{G_{\mathrm{BK},k} \times 10^{-12}}{A_k} = 1.16 \times 10^3\ \Omega^{-1}\mathrm{m}^{-2} \tag{40}$$

Additional Equations

Synaptic Cleft

Cl concentration (times the SC volume-area ratio R_s; in μM m):

$$N_{\mathrm{Cl},s} = N_{\mathrm{Na},s} + N_{\mathrm{K},s} - N_{HCO_{3,s}}\,; \quad [\mathrm{Cl}^-]_s = \frac{N_{\mathrm{Cl},s}}{R_s} \tag{41}$$

F	Faraday's constant	9.649×10^4 C mol^{-1}	
R_{gas}	Gas constant	8.315 J mol^{-1}K^{-1}	
T	Temperature	300 K	
g_{K_k}	Specific ion conductance of potassium	40×10^3 Ω^{-1}m^{-2}	[12]
$g_{\text{Na},k}$	Specific ion conductance of sodium	1.314×10^3 Ω^{-1}m^{-2}	[12]
$g_{\text{NBC},k}$	Specific ion conductance of the NBC cotransporter	7.57×10^2 Ω^{-1}m^{-2}	[12]
$g_{\text{KCC1},k}$	Specific ion conductance of the KCC1 cotransporter	10 Ω^{-1}m^{-2}	[12]
$g_{\text{NKCC1},k}$	Specific ion conductance of the NKCC1 cotransporter	55.4 Ω^{-1}m^{-2}	[12]
$J_{\text{NaK,max}}$	Maximum flux through the NaKATPase pump	1.42×10^{-3} µM m s^{-1}	[12]
$G_{\text{BK},k}$	Potassium conductance of the BK channel	4.3×10^3 pS	[?]
C_{input}	Block function to switch the channel on and off	0 ; 1 [-]	
$K_{\text{Na},k}$	Michaelis-Menten constant	10^4 µM	
$K_{\text{K},s}$	Michaelis-Menten constant	1.5×10^3 µM	
C_{unit}	Unit converting factor	10^3	M.E.

Astrocyte

Membrane voltage of the AC (V):

$$v_k = \frac{g_{\text{Na},k}E_{\text{Na},k} + g_{\text{K},k}E_{\text{K},k} + g_{\text{Cl},k}E_{\text{Cl},k} + g_{\text{NBC},k}E_{\text{NBC},k} + g_{\text{BK},k}w_kE_{\text{BK},k} - J_{\text{NaK},k}FC_{\text{unit}}}{g_{\text{Na},k} + g_{\text{K},k} + g_{\text{Cl},k} + g_{\text{NBC},k} + g_{\text{BK},k}w_k} \tag{42}$$

Nernst potential for the potassium channel (in mV):

$$E_{\text{K},k} = \frac{R_{\text{gas}}T}{z_KF}ln\left(\frac{[\text{K}^+]_s}{[\text{K}^+]_k}\right) \tag{43}$$

Nernst potential for the sodium channel (in mV):

$$E_{\text{Na},k} = \frac{R_{\text{gas}}T}{z_{\text{Na}}F}ln\left(\frac{Na_s}{Na_k}\right) \tag{44}$$

Nernst potential for the chloride channel (in mV):

$$E_{\text{Cl},k} = \frac{R_{\text{gas}}T}{z_{\text{Cl}}F}ln\left(\frac{[\text{Cl}^-]_s}{[\text{Cl}^-]_k}\right) \tag{45}$$

Nernst potential for the NBC channel (in mV):

$$E_{\text{NBC},k} = \frac{R_{\text{gas}}T}{z_{NBC}F}ln\left(\frac{Na_s{HCO_3}_s^2}{Na_k{HCO_3}_k^2}\right) \tag{46}$$

Nernst potential for the BK channel (in mV):

$$E_{\mathrm{BK},k} = \frac{R_{\mathrm{gas}}T}{z_K F} \ln\left(\frac{[\mathrm{K}^+]_p}{[\mathrm{K}^+]_k}\right) \tag{47}$$

Equilibrium state BK-channel (-):

$$w_\infty = 0.5\left(1 + \tanh\left(\frac{v_k + v_6}{v_4}\right)\right) \tag{48}$$

Time constant associated with the opening of BK channels (in s^{-1}):

$$\phi_w = \psi_w \cosh\left(\frac{v_k + v_6}{2v_4}\right) \tag{49}$$

$g_{\mathrm{Cl},k}$	Specific ion conductance of chloride	0.879 $\Omega^{-1}\mathrm{m}^{-2}$	[12]
z_K	Valence of a potassium ion	1	
z_{Na}	Valence of a sodium ion	1	
z_{Cl}	Valence of a chloride ion	-1	
z_{NBC}	Effective valence of the NBC cotransporter complex	-1	
v_6	Voltage associated with the opening of half the population	22 mV or V???	[?]
v_4	A measure of the spread of the distribution of the open probability of the BK channel	14.5 mV or V???	[?]
ψ_w	A characteristic time for the open probability of the BK channel	2.664 s^{-1}	[?]

5.2 The Smooth Muscle Cell and Endothelial Cell Model

Conservation Equations

Smooth muscle cell

Cytosolic [Ca^{2+}] in the SMC (in µM):

$$\begin{aligned}\frac{\mathrm{d}[\mathrm{Ca}^{2+}]_i}{\mathrm{d}t} = {} & J_{\mathrm{IP}_3,i} - J_{\mathrm{upt},i} + J_{\mathrm{CICR}_i} - J_{\mathrm{extr},i} + J_{\mathrm{leak},i} \ldots \\ & -J_{\mathrm{VOCC},i} + J_{\mathrm{Na/Ca},i} + 0.1J_{\mathrm{stretch},i} + J^{SMC-EC}_{Ca^{2+}-coupling_i}\end{aligned} \tag{50}$$

[Ca^{2+}] in the SR of the SMC (in µM):

$$\frac{\mathrm{d}[\widehat{\mathrm{Ca}^{2+}}]_i}{\mathrm{d}t} = J_{\mathrm{upt},i} - J_{\mathrm{CICR}_i} - J_{\mathrm{leak},i} \tag{51}$$

Membrane potential of the SMC (in mV):

$$\frac{\mathrm{d}v_i}{\mathrm{d}t} = \gamma_i(-J_{\mathrm{Na/K},i} - J_{\mathrm{Cl},i} - 2J_{\mathrm{VOCC},i} - J_{\mathrm{Na/Ca},i} - J_{\mathrm{K},i} \ldots \\ -J_{\mathrm{stretch},i} - J_{\mathrm{KIR},i}) + V_{coupling_i}^{SMC-EC} \tag{52}$$

Open state probability of calcium-activated potassium channels (dim.less):

$$\frac{\mathrm{d}w_i}{\mathrm{d}t} = \lambda_i \left(K_{act_i} - w_i\right) \tag{53}$$

IP_3 concentration om the SMC (in µM):

$$\frac{\mathrm{d}[\mathrm{IP_3}]_i}{\mathrm{d}t} = J_{IP_3-coupling_i}^{SMC-EC} - J_{\mathrm{degr},i} \tag{54}$$

K^+ concentration in the SMC (in µM):

$$\frac{\mathrm{d}[\mathrm{K^+}]_i}{\mathrm{d}t} = J_{\mathrm{Na/K},i} - J_{\mathrm{KIR},i} - J_{\mathrm{K},i} \tag{55}$$

γ_i	Change in membrane potential by a scaling factor	1970 $\mathrm{mV\mu M^{-1}}$	[10]
λ_i	Rate constant for opening	45.0 s^{-1}	[10]

Endothelial cell

Cytosolic Ca^{2+} concentration in the EC (in µM):

$$\frac{\mathrm{d}[\mathrm{Ca^{2+}}]_j}{\mathrm{d}t} = J_{\mathrm{IP_3},j} - J_{\mathrm{upt},j} + J_{CICR_j} - J_{\mathrm{extr},j} \ldots \\ +J_{\mathrm{leak},j} + J_{cation_j} + J_{0_j} + J_{\mathrm{stretch},j} - J_{Ca^{2+}-coupling_j}^{SMC-EC} \tag{56}$$

Ca^{2+} concentration in the ER in the EC (in µM):

$$\frac{\mathrm{d}[\widehat{\mathrm{Ca^{2+}}}]_j}{\mathrm{d}t} = J_{\mathrm{upt},j} - J_{CICR_j} - J_{\mathrm{leak},j} \tag{57}$$

Membrane potential of the EC (in mV):

$$\frac{\mathrm{d}v_j}{\mathrm{d}t} = -\frac{1}{C_{m_j}}(J_{K_j} + J_{R_j}) + V_{coupling_j}^{SMC-EC} \tag{58}$$

IP_3 concentration of the EC (in µM):

$$\frac{\mathrm{d}[\mathrm{IP_3}]_j}{\mathrm{d}t} = J_{\mathrm{EC,IP_3}} - J_{\mathrm{degr},j} - J_{IP_3-coupling_j}^{SMC-EC} \tag{59}$$

C_{m_j}	Membrane capacitance	25.8 pF	[10]
J_{PLC}	PLC / IP_3 production rate	0.18 or 0.4 $\mu M\,s^{-1}$	[10]
J_{0_j}	Constant Ca2+ leak term (influx)	0.029 $\mu M\,s^{-1}$	[10]

Fluxes

Smooth muscle cell

Release of calcium from IP_3 sensitive stores in the SMC (in $\mu M\,s^{-1}$):

$$J_{\mathrm{IP_3},i} = F_i \frac{[\mathrm{IP_3}]_i^2}{K_{ri}^2 + [\mathrm{IP_3}]_i^2} \tag{60}$$

F_i	Maximal rate of activation-dependent calcium influx	0.23 $\mu M\,s^{-1}$	[10]
K_{ri}	Half-saturation constant for agonist-dependent calcium entry	1 µM	[10]

Uptake of calcium into the sarcoplasmic reticulum (in $\mu M\ s^{-1}$):

$$J_{\mathrm{upt},i} = B_i \frac{{[\mathrm{Ca^{2+}}]_i}^2}{c_{bi}^2 + {[\mathrm{Ca^{2+}}]_i}^2} \tag{61}$$

B_i	SR uptake rate constant	2.025 $\mu M\ s^{-1}$	[10]
c_{bi}	Half-point of the SR ATPase activation sigmoidal	1.0 µM	[10]

Calcium-induced calcium release (CICR; in $\mu M\ s^{-1}$):

$$J_{\mathrm{CICR}_i} = C_i \frac{{[\widehat{\mathrm{Ca^{2+}}}]_i}^2}{s_{ci}^2 + {[\widehat{\mathrm{Ca^{2+}}}]_i}^2} \frac{{[\mathrm{Ca^{2+}}]_i}^4}{c_{ci}^4 + {[\mathrm{Ca^{2+}}]_i}^4} \tag{62}$$

C_i	CICR rate constant	55 $\mu M\ s^{-1}$	[10]
s_{ci}	Half-point of the CICR Ca^{2+} efflux sigmoidal	2.0 µM	[10]
c_{ci}	Half-point of the CICR activation sigmoidal	0.9 µM	[10]

Calcium extrusion by Ca^{2+}-ATPase pumps (in $\mu M\ s^{-1}$):

$$J_{\mathrm{extr},i} = D_i[\mathrm{Ca^{2+}}]_i \left(1 + \frac{v_i - v_d}{R_{di}}\right) \tag{63}$$

D_i	Rate constant for Ca^{2+} extrusion by the ATPase pump	0.24 s^{-1}	[10]
v_d	Intercept of voltage dependence of extrusion ATPase	-100.0 mV	[10]
R_{di}	Slope of voltage dependence of extrusion ATPase.	250.0 mV	[10]

Leak current from the SR (in µM s^{-1}):

$$J_{\text{leak},i} = L_i[\widehat{\text{Ca}^{2+}}]_i \tag{64}$$

L_i	Leak from SR rate constant	0.025 s^{-1}	[10]

Calcium influx through VOCCs (in µM s^{-1}):

$$J_{\text{VOCC},i} = G_{\text{Ca},i}\frac{v_i - v_{\text{Ca}_1,i}}{1 + \exp(-\left[\left(v_i - v_{\text{Ca}_2,i}\right)/R_{\text{Ca},i}\right])} \tag{65}$$

$G_{\text{Ca},i}$	Whole-cell conductance for VOCCs	1.29×10^{-3} µM $mV^{-1}s^{-1}$	[10]
$v_{\text{Ca}_1,i}$	Reversal potential for VOCCs	100.0 mV	[10]
$v_{\text{Ca}_2,i}$	Half-point of the VOCC activation sigmoidal	-24.0 mV	[10]
$R_{\text{Ca},i}$	Maximum slope of the VOCC activation sigmoidal	8.5 mV	[10]

Flux of calcium exchanging with sodium in the Na^+Ca^{2+} exchange (in µM s^{-1}):

$$J_{\mathrm{Na/Ca},i} = G_{\mathrm{Na/Ca},i} \frac{[\mathrm{Ca}^{2+}]_i}{[\mathrm{Ca}^{2+}]_i + c_{\mathrm{Na/Ca},i}} \left(v_i - v_{\mathrm{Na/Ca},i}\right) \tag{66}$$

$G_{\mathrm{Na/Ca},i}$	Whole-cell conductance for Na^+/Ca^{2+} exchange	3.16×10^{-3} µM $mV^{-1}s^{-1}$	[10]
$c_{\mathrm{Na/Ca},i}$	Half-point for activation of Na^+/Ca^{2+} exchange by Ca^{2+}	0.5 µM	[10]
$v_{\mathrm{Na/Ca},i}$	Reversal potential for the Na^+/Ca^{2+} exchanger	-30.0 mV	[10]

Calcium flux through the stretch-activated channels in the SMC (in µM s^{-1}):

$$J_{\mathrm{stretch},i} = \frac{G_{\mathrm{stretch}}}{1 + \exp\left(-\alpha_{\mathrm{stretch}}\left(\frac{\Delta p R}{h} - \sigma_0\right)\right)} \left(v_i - E_{\mathrm{SAC}}\right) \tag{67}$$

G_{stretch}	Whole cell conductance for SACs	6.1×10^{-3} µM $mV^{-1}s^{-1}$	[10]
$\alpha_{\mathrm{stretch}}$	Slope of stress dependence of the SAC activation sigmoidal	7.4×10^{-3} $mmHg^{-1}$	[10]
Δp	Pressure difference	30 mmHg	ME
σ_0	Half-point of the SAC activation sigmoidal	500 mmHg	[10]
E_{SAC}	Reversal potential for SACs	-18 mV	[10]

Flux through the sodium potassium pump (in µM s^{-1}):

$$J_{\mathrm{Na/K},i} = F_{\mathrm{Na/K},i} \tag{68}$$

$F_{\mathrm{Na/K},i}$	Rate of the potassium influx by the sodium potassium pump	4.32×10^{-2} µM s^{-1}	[10]

Chloride flux through the chloride channel (in µM s^{-1}):

$$J_{\mathrm{Cl},i} = G_{\mathrm{Cl},i}\left(v_i - v_{\mathrm{Cl},i}\right) \tag{69}$$

Potassium flux through potassium channel (in µM s^{-1}):

$$J_{\mathrm{K},i} = G_{\mathrm{K},i} w_i \left(v_i - v_{K_i}\right) \tag{70}$$

$G_{\mathrm{Cl},i}$	Whole-cell conductance for Cl^- current	1.34×10^{-3} µM $mV^{-1}s^{-1}$	[10]
$v_{\mathrm{Cl},i}$	Reversal potential for Cl^- channels.	-25.0 mV	[10]

$G_{\mathrm{K},i}$	Whole-cell conductance for K^+ efflux.	4.46×10^{-3} µM $mV^{-1}s^{-1}$	[10]
v_{K_i}	Nernst potential	-94 mV	[10]

Flux through KIR channels in the SMC (in µM s^{-1}):

$$J_{\mathrm{KIR},i} = \frac{F_{\mathrm{KIR},i} g_{\mathrm{KIR},i}}{\gamma_i}(v_i - v_{\mathrm{KIR},i}) \tag{71}$$

$F_{\mathrm{KIR},i}$	Scaling factor of potassium efflux through the KIR channel	750 mV μM^{-1}	[**?**]

IP_3 degradation (in µM s^{-1}):

$$J_{\mathrm{degr},i} = k_{\mathrm{d},i}[\mathrm{IP_3}]_i \tag{72}$$

$k_{\mathrm{d},i}$	Rate constant of IP_3 degradation	0.1 s^{-1}	[10]

Endothelial cell

Release of calcium from IP_3-sensitive stores in the EC (in µM s^{-1}):

$$J_{\mathrm{IP_3},j} = F_j \frac{[\mathrm{IP_3}]_j^2}{K_{rj}^2 + [\mathrm{IP_3}]_j^2} \tag{73}$$

F_j	Maximal rate of activation-dependent calcium influx	0.23 µM s^{-1}	[10]
K_{rj}	Half-saturation constant for agonist-dependent calcium entry	1 µM	[10]

Uptake of calcium into the endoplasmic reticulum (in µM s^{-1}):

$$J_{\mathrm{upt},j} = B_j \frac{{[\mathrm{Ca^{2+}}]_j}^2}{c_{bj}^2 + {[\mathrm{Ca^{2+}}]_j}^2} \tag{74}$$

B_j	ER uptake rate constant	0.5 µM s^{-1}	[10]
c_{bj}	Half-point of the SR ATPase activation sigmoidal	1.0 µM	[10]

Calcium-induced calcium release (CICR; in µM s^{-1}):

$$J_{CICR_j} = C_j \frac{\left[\widehat{\mathrm{Ca}^{2+}}\right]_j^{\,2}}{s_{cj}^2 + \left[\widehat{\mathrm{Ca}^{2+}}\right]_j^{\,2}} \frac{\left[\mathrm{Ca}^{2+}\right]_j^{\,4}}{c_{cj}^4 + \left[\mathrm{Ca}^{2+}\right]_j^{\,4}} \tag{75}$$

C_j	CICR rate constant	5 µM s^{-1}	[10]
s_{cj}	Half-point of the CICR Ca^{2+} efflux sigmoidal	2.0 µM	[10]
c_{cj}	Half-point of the CICR activation sigmoidal	0.9 µM	[10]

Calcium extrusion by Ca^{2+}-ATPase pumps (in µM s^{-1}):

$$J_{\mathrm{extr},j} = D_j[\mathrm{Ca}^{2+}]_j \tag{76}$$

D_j	Rate constant for Ca^{2+} extrusion by the ATPase pump	0.24 s^{-1}	[9]

Calcium flux through the stretch-activated channels in the EC (in µM s^{-1}):

$$J_{\mathrm{stretch},j} = \frac{G_{\mathrm{stretch}}}{1 + e^{-\alpha_{\mathrm{stretch}}(\sigma - \sigma_0)}} (v_j - E_{\mathrm{SAC}}) = \frac{G_{\mathrm{stretch}}}{1 + e^{-\alpha_{\mathrm{stretch}}\left(\frac{\Delta p R}{h} - \sigma_0\right)}} (v_j - E_{\mathrm{SAC}}) \tag{77}$$

G_{stretch}	The whole cell conductance for SACs	6.1×10^{-3} µM $mV^{-1}s^{-1}$	[10]
$\alpha_{\mathrm{stretch}}$	Slope of stress dependence of the SAC activation sigmoidal	7.4×10^{-3} $mmHg^{-1}$	[10]
Δp	Pressure difference	30 mmHg	ME
σ_0	Half-point of the SAC activation sigmoidal	500 mmHg	[10]
E_{SAC}	The reversal potential for SACs	-18 mV	[10]

table ist dop-pelt?!

Leak current from the ER (in µM s^{-1}):

$$J_{\mathrm{leak},j} = L_j[\widehat{\mathrm{Ca}^{2+}}]_j \tag{78}$$

L_j	Rate constant for Ca^{2+} leak from the ER	0.025 s^{-1}	[10]

Calcium influx through nonselective cation channels (in µM s^{-1}):

$$J_{cation_j} = G_{cat_j}(E_{Ca_j} - v_j)\frac{1}{2}\left(1 + \tanh\left(\frac{\log_{10}[Ca^{2+}]_j - m_{3_{cat_j}}}{m_{4_{cat_j}}}\right)\right) \tag{79}$$

G_{catj}	Whole-cell cation channel conductivity	6.6×10^{-4} µM $mV^{-1}s^{-1}$	[10]
E_{Caj}	Ca^{2+} equilibrium potential	50 mV	[10]
$m_{3_{catj}}$	Model constant	-0.18 µM	[10]
$m_{4_{catj}}$	Model constant	0.37 µM	[10]

Potassium efflux through the $J_{BK_{Caj}}$ channel and the $J_{SK_{Caj}}$ channel (in µM s^{-1}):

$$J_{K_j} = G_{totj}(v_j - v_{Kj})\left(J_{BK_{Caj}} + J_{SK_{Caj}}\right) \tag{80}$$

G_{totj}	Total potassium channel conductivity.	6927 pS	[10]
v_{Kj}	K^+ equilibrium potential	-80.0 mV	[10]

Potassium efflux through the $J_{BK_{Caj}}$ channel (in µM s^{-1}):

$$J_{BK_{Caj}} = 0.2\left(1 + \tanh\left(\frac{(\log_{10}[Ca^{2+}]_j - c)(v_j - b_j) - a_{1j}}{m_{3bj}(v_j + a_{2j}(\log_{10}[Ca^{2+}]_j - c) - b_j)^2 + m_{4bj}}\right)\right) \tag{81}$$

Potassium efflux through the $J_{SK_{Caj}}$ channel (in µM s^{-1}):

$$J_{SK_{Caj}} = 0.3\left(1 + \tanh\left(\frac{\log_{10}[Ca^{2+}]_j - m_{3sj}}{m_{4sj}}\right)\right) \tag{82}$$

Residual current regrouping chloride and sodium current flux (in µM s^{-1}):

$$J_{R_j} = G_{R_j}(v_j - v_{\text{rest},j}) \tag{83}$$

IP_3 degradation (in µM s^{-1}):

$$J_{\text{degr},j} = k_{\text{d},j}[IP_3]_j \tag{84}$$

c	Model constant, further explanation see reference	-0.4 µM	[10]
b_j	Model constant, further explanation see reference	-80.8 mV	[10]
a_{1j}	Model constant, further explanation see reference	53.3 µM mV	[10]
a_{2j}	Model constant, further explanation see reference	53.3 mVµM^{-1}	[10]
m_{3bj}	Model constant, further explanation see reference	1.32×10^{-3} µM mV^{-1}	[10]
m_{4bj}	Model constant, further explanation see reference	0.30 µM mV	[10]
m_{3sj}	Model constant, further explanation see reference	-0.28 µM	[10]
m_{4sj}	Model constant, further explanation see reference	0.389 µM	[10]

G_{R_j}	Residual current conductivity	955 pS	[10]
$v_{\text{rest},j}$	Membrane resting potential	-31.1 mV	[10]

$k_{\text{d},j}$	Rate constant of IP_3 degradation	0.1 s^{-1}	[10]

Coupling

Heterocellular electrical coupling between SMCs and ECs (in mV s^{-1}):

$$V_{coupling_i}^{SMC-EC} = -G_{coup}(v_i - v_j) \tag{85}$$

Heterocellular IP_3 coupling between SMCs and ECs (in µM s^{-1}):

$$J_{IP_3-coupling_i}^{SMC-EC} = -P_{IP_3}([\text{IP}_3]_i - [\text{IP}_3]_j) \tag{86}$$

Calcium coupling with EC (in µM s^{-1}):

$$J_{Ca^{2+}-coupling_i}^{SMC-EC} = -P_{Ca^{2+}}([\text{Ca}^{2+}]_i - [\text{Ca}^{2+}]_j) \tag{87}$$

G_{coup}	Heterocellular electrical coupling coefficient	0.5 s^{-1}	ME
P_{IP_3}	Heterocellular IP_3 coupling coefficient	0.05 s^{-1}	[10]
$P_{Ca^{2+}}$	Heterocellular $P_{Ca^{2+}}$ coupling coefficient	0.05 s^{-1}	[10]

Additional Equations

Equilibrium distribution of open channel states for the voltage and calcium activated potassium channels (dimensionless):

$$K_{act_i} = \frac{([\text{Ca}^{2+}]_i + c_{wi})^2}{([\text{Ca}^{2+}]_i + c_{wi})^2 + \beta_i \exp(-([v_i - v_{Ca_{3i}}]/R_{Ki}))} \tag{88}$$

Nernst potential of the KIR channel in the SMC (in mV):

$$v_{\mathrm{KIR},i} = z_1[\mathrm{K}^+]_p - z_2 \tag{89}$$

Conductance of KIR channel (in µM mV^{-1} s^{-1}):

$$g_{\mathrm{KIR},i} = \exp(z_5 v_i + z_3[\mathrm{K}^+]_p - z_4) \tag{90}$$

c_{wi}	Translation factor for Ca^{2+} dependence of K_{Ca} channel activation sigmoidal.	0.0 µM	[10]
β_i	Translation factor for membrane potential dependence of K_{Ca} channel activation sigmoidal.	0.13 μM^2	[10]
$v_{Ca_{3i}}$	Half-point for the K_{Ca} channel activation sigmoidal.	-27 mV	[10]
R_{Ki}	Maximum slope of the K_{Ca} activation sigmoidal.	12 mV	[10]
z_1	Model estimation for membrane voltage KIR channel	4.5×10^3 $\mathrm{mV\mu M^{-1}}$	[6]
z_2	Model estimation for membrane voltage KIR channel	112 mV	[6]
z_3	Model estimation for the KIR channel conductance	4.2×10^2 $\mathrm{mV^{-1}s^{-1}}$	[6]
z_4	Model estimation for the KIR channel conductance	12.6 µM $\mathrm{mV^{-1}s^{-1}}$	[6]
z_5	Model estimation for the KIR channel conductance	-7.4×10^{-2} µM $\mathrm{mV^{-2}s^{-1}}$	[6]

5.3 The Contraction Model

Fraction of free phosphorylated cross-bridges (dimensionless):

$$\frac{\mathrm{d}[Mp]}{\mathrm{d}t} = K_4[AMp] + K_1[M] - (K_2 + K_3)[Mp] \tag{91}$$

Fraction of attached phosphorylated cross-bridges (dimensionless):

$$\frac{\mathrm{d}[AMp]}{\mathrm{d}t} = K_3[Mp] + K_6[AM] - (K_4 + K_5)[AMp] \tag{92}$$

Fraction of attached dephosphorylated cross-bridges (dimensionless):

$$\frac{\mathrm{d}[AM]}{\mathrm{d}t} = K_5[AMp] - (K_7 + K_6)[AM] \tag{93}$$

Fraction of free non-phosphorylated cross-bridges (dimensionless):

$$[M] = 1 - [AM] - [AMp] - [Mp] \tag{94}$$

Rate constants that represent phosphorylation of M to Mp and of AM to AMp by the active myosin light chain kinase (MLCK), respectively (in s^{-1}):

$$K_1 = K_6 = \gamma_{cross}[\mathrm{Ca}^{2+}]_i^{\,n_{cross}} \tag{95}$$

K_2	Rate constant for dephosphorylation (of Mp to M) by myosin light-chain phosphatase (MLCP)	0.5 s^{-1}	[?]
K_3	Rate constants representing the attachment/detachment of fast cycling phosphorylated crossbridges	0.4 s^{-1}	[?]
K_4	Rate constants representing the attachment/detachment of fast cycling phosphorylated crossbridges	0.1 s^{-1}	[?]
K_5	Rate constant for dephosphorylation (of AMp to AM) by myosin light-chain phosphatase (MLCP)	0.5 s^{-1}	[?]
K_7	Rate constant for latch-bridge detachment	0.1 s^{-1}	[?]
γ_{cross}	Sensitivity of the contractile apparatus to calcium	17 μM^{-3} s^{-1}	[9]
n_{cross}	Fraction constant of the phosphorylation crossbridge	3 [–]	[9]

5.4 The Mechanical Model

Wall thickness of the vessel (in µm):

$$h = 0.1R \tag{96}$$

Fraction of attached myosin cross-bridges (dimensionless):

$$F_r = [AM_p] + [AM] \tag{97}$$

Vessel radius (in m):

$$\frac{\mathrm{d}R}{\mathrm{d}t} = \frac{R_{0_{pas}}}{\eta}\left(\frac{RP_T}{h} - E(F_r)\frac{R - R_0(F_r)}{R_0(F_r)}\right) \tag{98}$$

with:

$$E(F_r) = E_{pas} + F_r\left(E_{act} - E_{pas}\right) \tag{99}$$

$$R_0(F_r) = R_{0_{pas}} + F_r(\alpha_r - 1)R_{0_{pas}} \tag{100}$$

η	viscosity	10^4 Pa s	[10]
$R_{0_{pas}}$	Radius of the vessel when passive and no stress is applied	20 µm	ME
P_T	Transmural pressure	4×10^3 Pa	ME
E_{pas}	Young's modulus for the passive vessel	66×10^3 Pa	[7]
E_{act}	Young's modulus for the active vessel	233×10^3 Pa	[7]
α_r	Scaling factor initial radius	0.6	[7]

References

[1] **Donk, L. V. D. and Kock, E. G. J. D.** (**2013**): Bluefern Supercomputing Unit University of Canterbury Eindhoven University of Technology.

[2] **Dormanns, K.; Brown, R. G. and David, T.** (**2016**): The role of nitric oxide in neurovascular coupling, Journal of Theoretical Biology, Vol. 394 pp. 1–17.

[3] **Dunn, K. M.; Hill-Eubanks, D. C.; Liedtke, W. B. and Nelson, M. T.** (**2013**): TRPV4 channels stimulate Ca2+-induced Ca2+ release in astrocytic endfeet and amplify neurovascular coupling responses., Proceedings of the National Academy of Sciences of the United States of America, Vol. 110, No. 15 pp. 6157–62.

[4] **Farr, H. and David, T.** (**2011**): Models of neurovascular coupling via potassium and EET signalling, Journal of Theoretical Biology, Vol. 286, No. 1 pp. 13–23.

[5] **Filosa, J. A.** (**2004**): Calcium Dynamics in Cortical Astrocytes and Arterioles During Neurovascular Coupling, Circulation Research, Vol. 95, No. 10 pp. e73–e81.

[6] **Filosa, J. a.; Bonev, A. D.; Straub, S. V.; Meredith, A. L.; Wilkerson, M. K.; Aldrich, R. W. and Nelson, M. T.** (**2006**): Local potassium signaling couples neuronal activity to vasodilation in the brain, Nat Neurosci, Vol. 9, No. 11 pp. 1397–1403.

[7] **Gore, R. W. and Davis, M. J.** (**1985**): MECHANICS OF SMOOTH MUSCLE IN ISOLATED SINGLE MICROVESSELS, Vol. 12 pp. 511–520.

[8] **Hai, C. M. and Murphy, R. A.** (**1988**): Cross-bridge phosphorylation and regulation of latch state in smooth muscle Cross-bridge phosphorylation and regulation of latch state in smooth muscle, American Journal of Cell Physiology, Vol. 254 pp. C99——C106.

[9] **Koenigsberger, M.; Sauser, R.; Bény, J.-L. and Meister, J.-J.** (**2005**): Role of the endothelium on arterial vasomotion., Biophysical journal, Vol. 88, No. June pp. 3845–3854.

[10] **Koenigsberger, M.; Sauser, R.; Bény, J.-L. L. J. L. and Meister, J.-J. J. J.-J.** (**2006**): Effects of arterial wall stress on vasomotion, Biophysical journal, Vol. 91, No. September pp. 1663–1674.

[11] **Nagelhus, E.; Horio, Y. and Inanobe, A.** (**1999**): Immunogold evidence suggests that coupling of K+ siphoning and water transport in rat retinal muller cells is mediated by a coenrichment of kir4. 1 and aqp4 in specific membrane domains, Glia, Vol. 63, No. 1 pp. 47–54.

[12] **Østby, I.; Øyehaug, L.; Einevoll, G. T.; Nagelhus, E. a.; Plahte, E.; Zeuthen, T.; Lloyd, C. M.; Ottersen, O. P. and Omholt, S. W.** (**2009**): Astrocytic Mechanisms Explaining Neural-Activity-Induced Shrinkage of Extraneuronal Space, PLoS Computational Biology, Vol. 5, No. 1 p. e1000272.

[13] **Shipp, S.** (**2007**): Structure and function of the cerebral cortex., Current biology : CB, Vol. 17, No. 12 pp. R443———9.

[14] **Witthoft, A.; Em Karniadakis, G. and Karniadakis, G.** (**2012**): A bidirectional model for communication in the neurovascular unit., Journal of theoretical biology, Vol. 311 pp. 80–93.

[15] **Witthoft, A.; Filosa, J. A. and Karniadakis, G. E.** (**2013**): Potassium buffering in the neurovascular unit: Models and sensitivity analysis, Biophysical Journal, Vol. 105, No. 9 pp. 2046–2054.